

NJC

Accepted Manuscript



This is an *Accepted Manuscript*, which has been through the Royal Society of Chemistry peer review process and has been accepted for publication.

Accepted Manuscripts are published online shortly after acceptance, before technical editing, formatting and proof reading. Using this free service, authors can make their results available to the community, in citable form, before we publish the edited article. We will replace this *Accepted Manuscript* with the edited and formatted *Advance Article* as soon as it is available.

You can find more information about *Accepted Manuscripts* in the [Information for Authors](#).

Please note that technical editing may introduce minor changes to the text and/or graphics, which may alter content. The journal's standard [Terms & Conditions](#) and the [Ethical guidelines](#) still apply. In no event shall the Royal Society of Chemistry be held responsible for any errors or omissions in this *Accepted Manuscript* or any consequences arising from the use of any information it contains.



www.rsc.org/njc

ARTICLE

Synthesis and Characterization of Hexanuclear Copper-Yttrium Complex for Disposal to Semiconducting $\text{CuYO}_2\text{-}0.5\text{Cu}_2\text{O}$ Composite Thin Films[†]

Cite this: DOI: 10.1039/x0xx00000x

Received 00th January 2012,
Accepted 00th January 2012

DOI: 10.1039/x0xx00000x

www.rsc.org/

Sohail Ahmed,^a Muhammad Adil Mansoor,^a Wan Jeffrey Basirun,^{a,b} Mehran Sookhikian,^c Nay Ming Huang,^c LO Kong Mun,^a Tilo Söhnel,^{d,e} Zainudin Arifin,^a Muhammad Mazhar,^{*a}

The copper-yttrium hexanuclear complex $[\text{Cu}_4\text{Y}_2(\text{dmae})_6(\text{OAc})_{7.85}(\text{OH})_{0.15}(\text{H}_2\text{O})_2] \cdot 2\text{CH}_3\text{C}_6\text{H}_5$ (**1**) (where dmae = dimethylaminoethanoato, OAc = acetato) has been synthesized and characterized by melting point, elemental analysis, FT-IR, thermogravimetric/differential thermogravimetric (TG/DTG) and single crystal X-ray diffraction analysis. The complex crystallizes in the triclinic space group *P*-1 with cell parameters $a = 9.4934(3)$ Å, $b = 13.2045(4)$ Å, $c = 14.6990(5)$ Å, $\alpha = 76.486(2)^\circ$, $\beta = 85.811(2)^\circ$ and $\gamma = 83.394(2)^\circ$. A thin film of a $\text{CuYO}_2\text{-}0.5\text{Cu}_2\text{O}$ composite has been deposited on a FTO glass substrate by implementation of complex (**1**) at 400 °C under argon atmosphere by aerosol assisted chemical vapour deposition (AACVD). XRPD, SEM and EDX analysis reveal the formation of impurity-free crystallite mixtures of the $\text{CuYO}_2\text{-}0.5\text{Cu}_2\text{O}$ composite with well-defined evenly distributed rods of Cu_2O in the size range of 0.85 – 1.05 μm and granules of CuYO_2 in size range of 110 – 125 nm. UV-Vis spectrophotometric measurements and photoelectrochemical (PEC) results show an optical band gap energy of 2.6 eV and a photocurrent density of 81 μA/cm² under illumination by a 150 W halogen lamp at a potential of 1.0 V vs SCE.

Keywords: Synthesis, yttrium-copper oxide, semiconductor, nano composites, photoelectrochemical.

1. Introduction

The development of new synthetic strategies to assemble high-nuclearity transition metal complexes is a key target in modern coordination chemistry.^{1, 2} Heterometallic complexes have been extensively studied for many years. Complexes containing alkoxide and acetato ligands are of particular interest, partly due to their potential utility as molecular models for superconductors and in fabrication of thin films at low temperatures of 400-500 °C by using chemical vapour deposition (CVD).³⁻⁶ Multifunctional ligands such as alkoxido,

acetato, fluoroacetato and β-diketonato coordinatively saturate each metal atom and restrict its ability to oligomerize at the same time enhancing its solubility in organic solvents and making it useful as a precursor to fabricate bimetallic composite oxide thin films.⁷ Extensive work has been done on the development of heterometallic complexes of copper with yttrium and barium such as $[\text{Y}_2\text{Cu}_8(\mu\text{-PyO})_{12}(\mu\text{-Cl})_2(\mu_4\text{-O})_2(\text{NO}_3)_4(\text{H}_2\text{O})_2 \cdot 2\text{H}_2\text{O}]$,⁸ $[\text{Ba}(\text{Cu}[\text{OCMe}(\text{CF}_3)_2]_3)]$,⁹ $[\text{Y}_2\text{Cu}_8\text{O}_2(\text{PyO})_{12}\text{C}_{12}(\text{NO}_3)_4(\text{H}_2\text{O})_2]$,¹⁰ $([\text{Ba}_3\text{Cu}_2(\text{CF}_3\text{CO}_2)_6(\text{Me}_2\text{NC}_2\text{H}_4\text{O})_4(\text{MeOH})_2]_2\text{MeOH})$,¹¹ $[\text{BaCu}_4(\text{PyO})_4(\text{bdmap})_4(\text{O}_2\text{CCF}_3)_2]$,

[BaCu₄(PyO)₄(deae)₄(O₂CCF₃)₂],¹² [BaCu(C₂H₆O₂)₆(C₂H₄O₂)₂] and [BaCu(C₂H₆O₂)₃(C₂H₄O₂)₂],¹³ but none of these compounds has been investigated for their implementation as a precursor for chemical vapour deposition of Cu-Y ceramic oxides. Various synthetic techniques have been adopted for the fabrication of mixed metal ceramic oxide thin films. However, the use of single source molecular precursors in aerosol assisted chemical vapour deposition (AACVD) is gaining more attention because it provides advantages such as excellent film uniformity, high deposition rates, control over material composition and phase, conformal coverage on complex geometries, controllability of film microstructures, low-cost and scalability.

In continuation of our efforts directed towards the development of bi- and tri heterometallic complexes^{14, 15}, we report herein a novel structured heterobimetallic complex [Cu₄Y₂(dmae)₆(OAc)_{7.85}(OH)_{0.15}(H₂O)₂]·2CH₃C₆H₅ (**1**) as a single source molecular precursor for the fabrication of impurity-free CuYO₂-0.5Cu₂O composite thin film using the AACVD technique at 400 °C. The deposited films were characterized by XRPD, FESEM, EDX and UV-visible spectrophotometry for their stoichiometry, morphology, thickness and optical band gap. Further scope of these thin films for application in photoelectrochemical water splitting to hydrogen and oxygen is also investigated.

2. Experimental

2.1. Material and Methods

All experiments were carried out under an inert atmosphere of dry argon gas using Schlenk tubes and inert gas line. All solvents were purchased from Fluka. Toluene was rigorously dried over sodium benzophenone and methanol was purified by distilling over reagent grade magnesium powder. N,N-dimethylaminoethanol (dmaeH) was purchased from Aldrich, purified by refluxing over K₂CO₃ for 10 h and distilled immediately before use. The melting point was determined in a capillary tube using an electrothermal melting point apparatus, model MP.D Mitamura Riken Kogyo (Japan) and is uncorrected. The microanalyses were performed using a Leco CHNS 932. FT-IR spectra were recorded on a single reflectance ATR instrument (4000–400 cm⁻¹, resolution 4 cm⁻¹). The controlled thermal analysis was investigated using a Mettler Toledo TGA/SDTA 851e Thermogravimetric Analyzer. The thermal measurements were carried out in an alumina crucible under an atmosphere of flowing nitrogen gas (50 cm³ min⁻¹) with a heating rate of 20 °C/min.

2.2. Synthesis of



0.035 g (0.39 mmol) N,N-dimethylaminoethanol (dmaeH) was injected slowly to 0.050 g (0.39 mmol) copper methoxide placed in 50 mL Schlenk tube fitted with a vacuum/Ar gas line and magnetic stirrer. The reaction mixture was stirred slowly under vacuum for 2 hours to evacuate the methanol formed and any unreacted dmaeH. The residual paste was dissolved in 5 mL of toluene and extracted from unreacted copper (II) methoxide by cannula filtration. At this stage 0.10 g Y(OAc)₃·xH₂O suspended in 25 mL of toluene was added drop wise with vigorous stirring that continued for 5 h. Filtration through cannula gave a clear light blue solution which was evaporated to dryness under vacuum. The solid was washed

three times with 5 mL dry n-hexane and re-dissolved in 3 mL of dry toluene to harvest the first crop of light blue crystals after 5 days at -10 °C. Yield 58%, m.p. 142 °C, microanalysis: % calculated(found)

for [Cu₄Y₂(dmae)₆(OAc)_{7.85}(OH)_{0.15}(H₂O)₂]·2CH₃C₆H₅ (formula weight: 1647.00): C, 39.1 (35.9); H, 6.3 (6.4); N, 5.1 (4.7), FT-IR (cm⁻¹): 2976(w), 2865(m), 1571s, 1425s, 1396s, 1335w, 1272m, 1073 (m), 1018(m), 505 (m), 467 (w). TGA: Temperature (%weight loss) 150 °C (10.7); 150 – 243.7 °C (42.9) and 243.73 – 380.7 °C (65.9).

Single crystal XRD measurements were performed on a CCD diffractometer (Bruker Smart APEXII) with graphite-monochromatized Mo K α radiation, $\lambda_{\text{Mo}} = 0.71073$ Å. Data reduction was carried out using the SAINT¹⁶ program. Semi-empirical absorption corrections were applied based on equivalent reflections using SADABS.¹⁷ The structure solution and refinements were performed with SHELXS-2013 and SHELXL-2013 program packages.¹⁸

2.3. Deposition of thin films by AACVD

The thin films of composite oxides were deposited on commercially available FTO-coated glass substrates using self-designed AACVD assembly as described elsewhere.¹⁹ FTO-coated glass substrates of size 2 x 1 cm (L x W) purchased from Sigma Aldrich were cleaned by ultrasonic washing with distilled water, acetone, and ethyl alcohol prior to their use. Finally, they were washed with distilled water, stored in ethanol and dried in air. Substrate slides were placed inside the tube furnace and then heated up to the deposition temperature for 10 min before carrying out the deposition. The aerosol of the precursor solution was formed by keeping the round bottom flask in a water bath above the piezoelectric modulator of an ultrasonic humidifier. The generated aerosol droplets of the precursor were transferred into the hot wall zone of the reactor by flowing nitrogen gas. At the end of the deposition, the aerosol line was closed and the carrier gas passed over the substrate to cool to room temperature before it was taken out from the reactor. In a typical experiment, 16.5 mg of the precursor (**1**) was dissolved in 50 mL of toluene to deposit thin films of composite CuYO₂-0.5Cu₂O on FTO-coated conducting glass substrate under argon with a flow rate of 150 cm³ min⁻¹ at 400 °C. The deposited thin films are light yellow in colour, transparent, uniform, robust, and stable towards atmospheric conditions and adhere strongly on the FTO substrate as verified by the "Scotch tape test".²⁰

2.3.1. Characterization of thin films

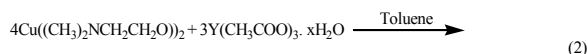
The surface morphology of thin films was studied using a field-emission gun scanning electron microscope (FESEM, FEI Quanta 400) coupled with Energy Dispersive X-ray spectrometer EDX (INCA Energy 200 (Oxford Inst.), at an accelerating voltage of 10 kV, and a working distance of 6 mm. The final products were characterised by using powder X-ray diffraction (PXRD) on a D8 Advance X-Ray Diffractometer (Bruker AXS) using CuK α radiation ($\lambda = 1.540$ Å), at a voltage of 40 kV and current of 40 mA at ambient temperature. The optical absorption spectrum of the thin films was recorded on a Lambda 35 Perkin-Elmer UV-visible spectrophotometer in the wavelength range of 450-700 nm. The thickness of the films was measured by profilometer KLA Tencore P-6 surface profiler. The photo-electrochemical response of the fabricated CuYO₂-0.5Cu₂O thin film was studied by linear scanning voltammetry (LSV) in the absence and presence of light (150

W halogen lamp). A three-compartment cell with a saturated calomel electrode (SCE) as the reference (RE), $\text{CuYO}_2\text{-}0.5\text{Cu}_2\text{O/FTO}$ ($0.5 \times 1 \times 1$ cm) as the working electrode (WE), and a Pt wire as the counter electrode (CE) were used in the photocurrent measurements. A general purpose electrochemical software (GPES) installed in a computer and interfaced with the Auto-lab PGSTAT-302N (Ecochemie, Netherlands) potentiostat/galvanostat was used to run the experiments. The scan rate for LSV was 25 mV s^{-1} between 0.0 V to 1.5 V in 0.1 M phosphate buffer solution at pH 7.2.

3. Results and discussion

3.1. Synthesis and Characterization

The hexanuclear complex $[\text{Cu}_4\text{Y}_2(\text{dmae})_6(\text{OAc})_{7.85}(\text{OH})_{0.15}(\text{H}_2\text{O})_2] \cdot 2\text{CH}_3\text{C}_6\text{H}_5$ (**1**) (dmae = dimethylethanolamino, OAc = acetato) has been synthesized in 58% yield by a direct condensation reaction between dimethoxycuprate(II) with dmaeH as shown in chemical equation 1. The reaction proceeds smoothly without solvent and any unreacted dmaeH and methanol formed during reaction is removed under vacuum to yield sticky material, which was dissolved in dry toluene and filtered into a flask containing stirred $\text{Y}(\text{acetate})_3 \cdot x\text{H}_2\text{O}$ suspension in toluene. The completion of the reaction was indicated by the disappearance of the solid and the formation of a bright blue coloured solution (chemical equation 2).



The complex (**1**) (m.p. 142°C) is soluble in toluene, chloroform and tetrahydrofuran and is stable in air under normal atmospheric conditions. The stoichiometry of the complex (**1**) was first determined by single crystal X-ray analysis and was further verified by micro-analysis and FT-IR. Microanalysis indicates that the percentage hydrogen and nitrogen in the complex are in good agreement with the expected values while carbon is bit off the theoretical value probably due to solvated toluene molecules that can be easily lost during storage. In the FT-IR spectrum, a broad absorption band at 3343 cm^{-1} is due to an OH group and coordinated H_2O molecules; the presence of both carboxylato and aminoalcoholato ligands in the complex were also identified by their vibrational signals. The anti-symmetric and symmetric stretching vibrations for CO_2 were assigned at 1571 cm^{-1} and 1425 cm^{-1} respectively.²¹ The difference of 146 cm^{-1} between the anti-symmetric and symmetric stretching vibrations suggests a chelating or bridging-chelating behaviour for carboxylate ligands.^{22, 23} The presence of three strong absorption bands in the range of $1173\text{-}1272 \text{ cm}^{-1}$ for $\nu(\text{C-O})$ stretching corresponds to carboxylato ligands.²⁴ The absorptions at low frequency of 591 and 467 cm^{-1} are probably due to Cu-O and Cu-N stretching vibrations respectively.^{25, 26}

3.2. Structural analysis of

$[\text{Cu}_4\text{Y}_2(\text{dmae})_6(\text{OAc})_{7.85}(\text{OH})_{0.15}(\text{H}_2\text{O})_2] \cdot 2\text{CH}_3\text{C}_6\text{H}_5$ (**1**)

The molecular structure of the Cu-Y complex is shown in Fig. 1 and the crystal geometry at the copper and yttrium metal centres is depicted in Fig. 2. The molecule lies on a centre of inversion and consists of four copper and two yttrium metal

centres. The two symmetry related half units are linked together by two carboxylate bridges. Each symmetry related half unit consists of two copper atoms and one yttrium atom and they are linked together by two μ^2 -2-(dimethyl aminoethanolato) ligands and one μ^3 -(2-dimethylaminoethanolato) ligand. Cu(1) is 5-fold coordinated with a distorted square pyramidal geometry. The square plane is formed by two oxygen atoms from the (2-dimethylaminoethanolato) ligands, one monodentate carboxylato ligand and the nitrogen atom of a μ^2 -2-dimethylaminoethanolato ligand while the axial position is occupied by a bidentate carboxylato oxygen atom. The distortion from ideal square pyramidal geometry is evident from the sum of angles subtended at the metal centre which is 358.66° . Cu(2) is also 5-fold coordinated but its geometry is best described as a distorted trigonal bipyramid, with the equatorial trigonal plane occupied by two nitrogen atoms from the (2-dimethylaminoethanolato) ligands and one (2-dimethylaminoethanolato) oxygen atom, while the oxygen atom of the other (2-dimethylaminoethanolato) ligand and the bidentate carboxylato oxygen atom complete the axial position of the trigonal bipyramidal geometry. The distortion is seen from the sum of angles subtended at the copper centre being 358.51° and the O-Cu-O angle at the axial position of $175.82(7)^\circ$. The bidentate carboxylato moiety bonds to two copper atoms with unequal Cu-O bond distances, (Cu(2)-O(5) = $1.948(2) \text{ \AA}$), while Cu(1)-O(4) = $2.265(2) \text{ \AA}$ clearly shows that the carbonyl oxygen atom is weakly coordinated to Cu(1). The monodentate carboxylate ligand is bonded to Cu1 with Cu(1)-O(8) bond distance of $1.947(2) \text{ \AA}$, similar to that of Cu(2)-O(5) and other Cu-O bond distances of similar compounds.²⁷

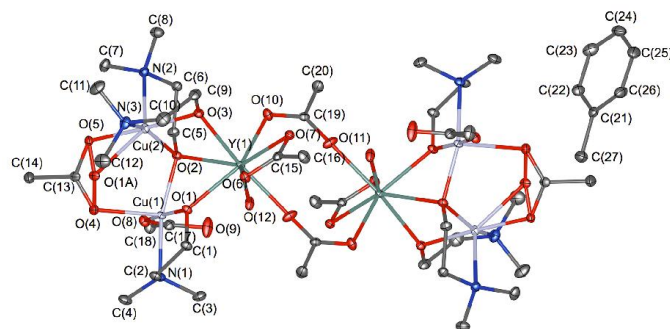


Figure 1 The molecular structure of complex (**1**) showing 35% probability displacement ellipsoids and the atom numbering. Hydrogen atoms are omitted.

The yttrium atom, on the other hand, is 8-fold coordinated with three (2-dimethylaminoethanolato) oxygen atoms. Two oxygen atoms of the bridging carboxylates, two oxygen atoms of the intramolecularly coordinated bidentate carboxylate and a water molecule complete the coordination sphere. The bidentate carboxylate ligand coordinates to the yttrium atom with unequal Y-O bond distances [Y(1)-O(7) = $2.409(2) \text{ \AA}$ and Y(1)-O(6) = $2.490(2) \text{ \AA}$]. The water molecule which is coordinated to the yttrium atom [Y(1)-O(12) = $2.369(2) \text{ \AA}$] is also hydrogen-bonded to the monodentate carboxylate oxygen (O(12)-H...O(9) = $2.622(4) \text{ \AA}$) and the oxygen of the bidentate carboxylate (O(12)-H...O(7) $2.756(3) \text{ \AA}$) of the symmetry related half fragment.

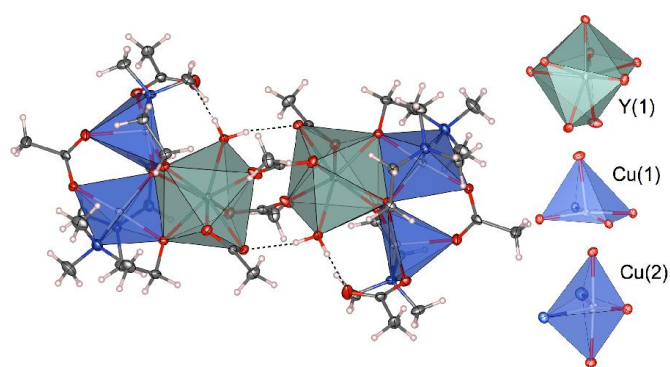


Figure 2 Molecular structure of complex (**1**) showing the geometry at the four copper (purple) and two yttrium (grey) metal centres. O(1A) atoms omitted for clarity.

In the crystal structure the molecules are stacked along [100] forming a channel structure. Toluene molecules fill the channels which show weak hydrogen bonding (C(X)-H...O(X) = 3.346(4) Å) to one carboxylate ligand. There is no intermolecular hydrogen bonding between the Y-Cu complexes (Fig. 3).

The bridging carboxylate ligand, which is bonded to the two copper atoms, was refined to a chemical occupancy of 92.5(3)% while the other 7.5(3)% was occupied by a hydroxyl bridge [O(1a)-Cu(1) = 2.69(3) Å and O(1A)-Cu(2) = 2.29(3) Å].

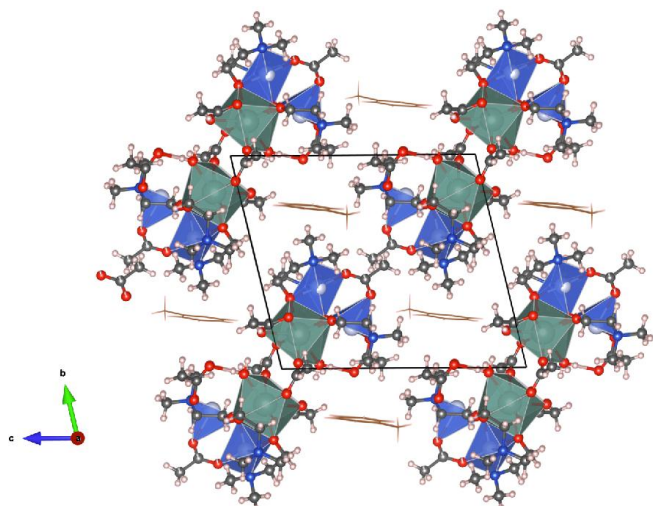


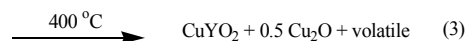
Figure 3 Crystal structure of complex (**1**); toluene molecules are shown as wireframe models in channels formed by **1**; O(1A) omitted for clarity.

Table 1. Selected bond distances and bond angles of complex (**1**)

Metal-Metal bond distances [Å]			
Y(1)-O(1)	2.2769(14)	Cu(1)-N(1)	2.050(2)
Y(1)-O(2)	2.5187(14)	Cu(2)-N(2)	2.344(2)
Y(1)-O(3)	2.2868(14)	Cu(2)-N(3)	2.055(2)
Y(1)-Cu(1)	3.3135(3)	Cu(1)-O(4)	2.266(2)
Y(1)-Cu(2)	3.3176(3)	C(2)-O(2)	2.024(1)
Bond angles [°]			
O(1)-Y(1)-Cu(1)	34.82(3)	O(1)-Cu(1)-Y(1)	41.99(4)
O(3)-Y(1)-Cu(1)	92.15(4)	O(2)-Cu(1)-Y(1)	49.31(4)
O(1)-Y(1)-O(2)	63.51(5)	O(4)-Cu(1)-Y(1)	126.76(4)
O(1)-Y(1)-O(3)	87.55(5)	Cu(1)-Y(1)-Cu(2)	57.547(7)
O(1)-Y(1)-O(6)	77.28(5)	Y(1)-Cu(2)-N(1)	113.62(5)
		Cu(1)-Y(1)-Cu(2)	

3.3. Thermal Studies of Complex (**1**)

Thermal properties are important for the application of molecular complexes as precursors to ceramic materials, since they determine the processing temperature, reaction atmosphere and composition of the targeted material. The thermal behaviour of (**1**) has been analysed by thermogravimetric analysis implemented under an inert atmosphere of flowing nitrogen gas (25 cm³/min) with a heating rate of 20 °C/min. The DTG of the precursor (**1**) shows three distinct endothermic signals at 150 °C, 243.7 °C and 380.7 °C (Fig. 4) during the thermal pyrolysis process. The TG shows that the thermal degradation of (**1**) begins slowly with the loss of two solvent toluene molecules at 150 °C. The second decomposition step of the complex takes place in the temperature range of 150 – 243.7 °C corresponding to a weight loss of 42.9% of total mass of complex (**1**). This weight loss is attributed to the loss of two water molecules, 0.15 hydroxyl and 7.85 acetato molecules, respectively. The termination of weight loss occurs by the removal of the remaining six dmae groups at 380.7 °C leaving behind CuYO₂-0.5Cu₂O composite amounting to 34.1% of the original mass of complex (**1**) as shown in chemical equation 3. Further heating of the residue to 900 °C did not bring any change in weight indicating that the complex (**1**) has completely collapsed to the composite CuYO₂-0.5Cu₂O. The FTIR of the residue did not show any absorption due to acetate or dmae ligands suggesting complete removal of the entire organic component from the composite. Further, two IR absorption bands of residue appeared at 599 and 534 cm⁻¹ confirm the presence Cu₂O²⁸ and Y₂O₃^{29, 30} moieties respectively in the composite.



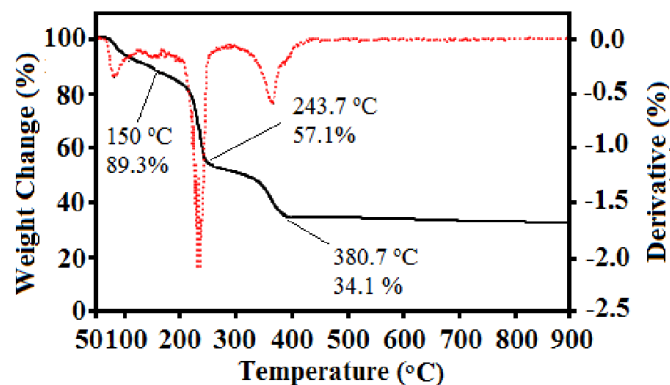


Figure 4 TGA/DTG curves recorded under an inert nitrogen ambient showing pyrolysis of complex (**1**) at gas flow rate of 25 cm³/min and heating rate of 20 °C/min.

3.4. Powder X-ray diffraction studies of thin films

The powder diffraction pattern of CuYO₂-0.5Cu₂O nano composite thin films deposited on FTO matches very well with JCPDS card No [00-037-0929] and [00-001-1142] for the hexagonal phase of CuYO₂ and cubic phase of Cu₂O respectively. The CuYO₂-0.5Cu₂O composite thin films crystallizes in a hexagonal crystal system (space group *P6₃/mmc*) with cell parameters of *a* = 3.5206 Å, *c* = 11.4180 Å. Cu₂O is cubic having the space group *Pn-3m* with cell parameter *a* = 4.252 Å. The relative intensities and the position of the diffraction peaks are shown in Fig. 5. XRD peaks at 2θ value of 51.90, 54.50, 61.87 and 65.32° correspond respectively to (110), (112), (114) and (008) lattice reflection planes of the hexagonal CuYO₂ phase, whereas peaks at 2θ value of 29.76, 36.65 and 42.61° correspond respectively to (110), (111) and (200) lattice reflection planes of the cubic Cu₂O phase. XRD peaks of impurities are not observed, which indicates the high purity of the samples. The crystal size of CuYO₂ estimated to be 57.5 nm calculated from Scherer's equation.

3.5 Surface Morphology

Fig. 6 shows the SEM image of the surface of the composite CuYO₂-0.5Cu₂O thin films grown on FTO glass at 400 °C. The photomicrograph indicates uniformly distributed Cu₂O rods of various length ranging from 0.85-1.05 μm and CuYO₂ granules in the size range of 110-125 nm in the composite. Most of the Cu₂O rods are grown in all directions while CuYO₂ nanoparticles are accumulated at the ends of the rods leaving some of the regions void.

The EDX analysis (Figure S2) affirms the presence of copper, yttrium and oxygen in the deposited films. The atomic ratio of Cu : Y in the films is 2 : 0.95 which is in accordance with the expected 2 : 1 elemental ratio present in complex (**1**).

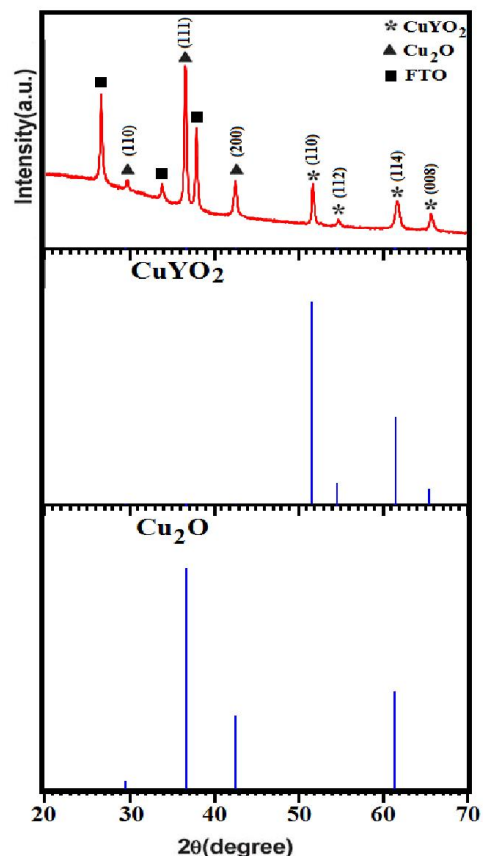


Figure 5 Comparison of XRD powder pattern of CuYO₂-0.5Cu₂O composite thin films deposited from precursor (**1**) at 400 °C in an atmosphere of nitrogen for 45 minutes, with standard peak pattern of CuYO₂ and Cu₂O.

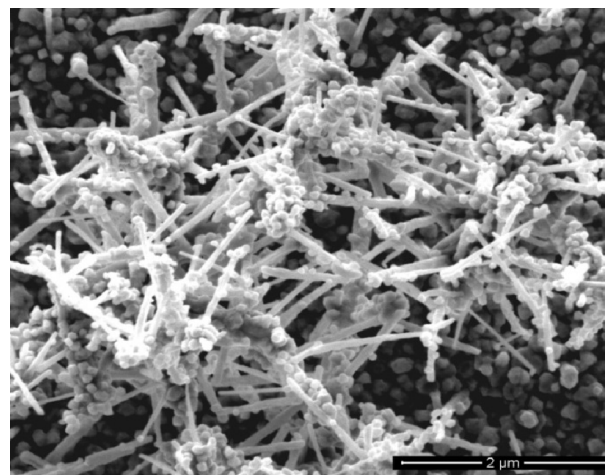


Figure 6 shows photomicrographs of CuYO₂-0.5Cu₂O composite thin films from complex (**1**) grown on FTO glass substrates at 400 °C in an atmosphere of nitrogen for 45 minutes.

3.6. Optical band gap

The optical absorption spectrum of the composite $\text{CuYO}_2\text{-}0.5\text{Cu}_2\text{O}$ thin films was recorded on a Lambda 35 Perkin-Elmer UV-Vis spectrophotometer in the wavelength range of 450-700 nm using similar FTO coated glass substrate as a reference to exclude the substrate contribution in the spectrum. The UV-Vis spectrum of $\text{CuYO}_2\text{-}0.5\text{Cu}_2\text{O}$ thin film shows an absorption edge at 455.5 nm and the band gap was calculated by plotting Tauc plot³¹ of energy versus $(\alpha h\nu)^2$ to give a value of 2.6 eV as given in Fig 7. It is reported that the optical band gap of Cu_2O is 2.1 eV.³² In contrast, the band gap of the composite $\text{CuYO}_2\text{-}0.5\text{Cu}_2\text{O}$ is 2.6 eV which is in accordance with the known fact that band gaps are seriously affected by the addition of dopants and composite formation.³³

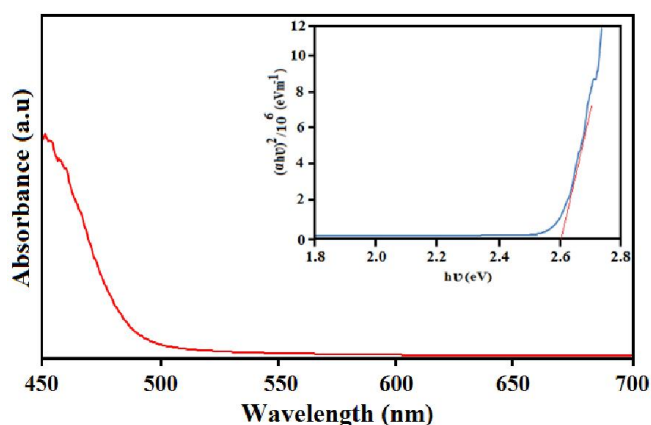


Figure 7 UV-Vis spectrum of wavelength versus absorbance and inset Tauc plot of energy versus $(\alpha h\nu)^2$ of $\text{CuYO}_2\text{-}0.5\text{Cu}_2\text{O}$ thin films deposited from precursor **(1)** using AACVD.

3.7. Photoelectrochemical studies

The current-potential diagram of a $\text{CuYO}_2\text{-}0.5\text{Cu}_2\text{O}$ electrode in the dark and under irradiation is shown in Fig. 8, which shows that the LSV of $\text{CuYO}_2\text{-}0.5\text{Cu}_2\text{O}$ film has higher current under illumination compared to the dark. When illuminated, electrons are excited to the conduction band and leaving holes in the valence band of the photo-anode, where water oxidation occurs as follows³³

$$2\text{H}_2\text{O} + 4\text{h}^+ \rightarrow 4\text{H}^+ + \text{O}_2 \quad (1)$$

The current increases with illumination compared to the dark at potentials beyond 1 V vs SCE, or 1.23 V vs SHE, which is the equilibrium potential for water electrolysis (the equilibrium potential of SCE is 0.24 V vs SHE).



Lower than 1.0 V vs. SCE, the currents under illumination and the dark are almost the same. The electrons that reach the platinum counter electrode are used for hydrogen production.^{34, 35} Beyond 1 V vs. SCE, it was observed that gas bubbles were released from the platinum counter electrode.

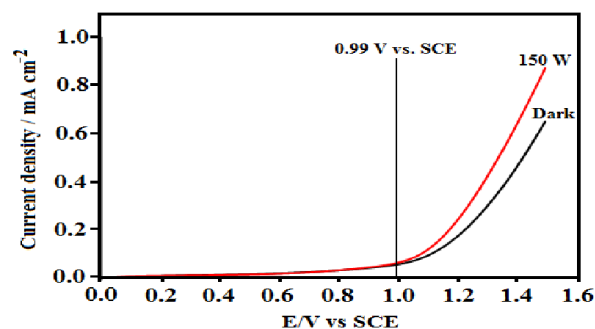
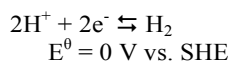
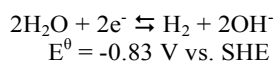


Figure 8 LSV of $\text{CuYO}_2\text{-}0.5\text{Cu}_2\text{O}$ composite thin film at an optimum deposition temperature of 400 °C, deposition time of 50 min, and 0.1 M solution of complex **(1)** in toluene; under illuminated (150 W) and dark (D) conditions.

In summary, the $\text{CuYO}_2\text{-}0.5\text{Cu}_2\text{O}$ composite prepared from precursor **(1)** has a narrow range of visible light absorption and optical band gap of 2.6 eV indicating its limited ability to harvest solar light. However the complex and composite seems to have a potential for application as an intermediate for the synthesis of various yttrium, barium and copper based superconductors.

4. Conclusions

In summary this contribution reports an easily synthesized Cu-Y bimetallic complex $[\text{Cu}_4\text{Y}_2(\text{dmae})_6(\text{OAc})_{7.85}(\text{OH})_{0.15}(\text{H}_2\text{O})_2] \cdot 2\text{CH}_3\text{C}_6\text{H}_5$ **(1)** and disposed it as a clean precursor to crystalline composite $\text{CuYO}_2\text{-}0.5\text{Cu}_2\text{O}$ thin films by AACVD. The compositional analysis and study of photoelectrochemical measurements of the deposited films indicate possible use of the complex towards synthesis of Cu-Y based superconductors and for the preparation of materials for application in photo-electronic devices.

Acknowledgements

M.M and HNM acknowledge the University of Malaya for its generous financial support through UMRG grant no. UM.TNC2/RC/261/1/1/RP007A/B-13AET; High Impact Research Grant (UM.C/625/1/ HIR/242 and UM.C/625/1/HIR/MOHE/SC/21).

Notes and references

^aDepartment of Chemistry, Faculty of Science, University of Malaya, Kuala Lumpur 50603, Malaysia. Phone: +60379674269 Email: mazhar42pk@yahoo.com.

^bInstitute of Nanotechnology and Catalysis (NanoCat), Institute of Postgraduate Studies, University of Malaya, 50603, Kuala Lumpur, Malaysia.

^cLow Dimensional Materials Research Centre, Department of Physics, University of Malaya, Faculty of Science, Kuala Lumpur 50603, Malaysia.

^dSchool of Chemical Sciences, The University of Auckland, Private Bag 92019, Auckland, New Zealand

^eCentre for Theoretical Chemistry and Physics, The New Zealand Institute for Advanced Study, Massey University Auckland, New Zealand.

†CCDC1009779 contains the supplementary crystallographic data for this paper. These data can be obtained free of charge via <http://ccdc.cam.ac.uk/conts/retrieving.html> or from the Cambridge Crystallographic Data centre, 12 Union Road, Cambridge CB2 1EZ, UK; fax: (+44) 1223 336 033; or email : deposit@ccdc.cam.ac.uk.

Electronic Supplementary Information (ESI) available: [Supporting figures for FTIR and EDX are available in ESI]. See DOI: 10.1039/b000000x/

1. K. G. U. W. a. D. H. Auty, in *Encyclopaedia of Materials: Science and Technology*, Elsevier, Oxford, 2008, p. 5.
2. A. Glass John, S. Kher Shreyas, Y. Tan and T. Spencer James, in *Inorganic Materials Synthesis*, American Chemical Society, 1999, vol. 727, pp. 130-143.
3. M. A. Mansoor, A. Ismail, R. Yahya, Z. Arifin, E. R. T. Tiekink, N. S. Weng, M. Mazhar and A. R. Esmaili, *Inorg. Chem.*, 2013, **52**, 5624-5626.
4. A. C. Jones, *J. Mater. Chem.*, 2002, **12**, 2576-2590.
5. S. Basharat, C. J. Carmalt, R. Binions, R. Palgrave and I. P. Parkin, *Dalton Trans.*, 2008, 591-595.
6. C. E. Knapp, G. Hyett, I. P. Parkin and C. J. Carmalt, *Chem. Mater.*, 2011, **23**, 1719-1726.
7. M. Shahid, M. Mazhar, M. Hamid, M. Zeller, P. O'Brien, M. A. Malik, J. Raftery and A. D. Hunter, *New J. Chem.*, 2009, **33**, 2241-2247.
8. S. Wang, *Inorg. Chem.*, 1991, **30**, 2252-2253.
9. A. P. Purdy and C. F. George, *Inorg. Chem.*, 1991, **30**, 1969-1970.
10. S. Wang, Z. Pang and M. J. Wagner, *Inorg. Chem.*, 1992, **31**, 5381-5388.
11. J. Zhang, L. G. Hubert-Pfalzgraf and D. Luneau, *Inorg. Chem. Commun.*, 2004, **7**, 979-984.
12. S. Wang, S. J. Trepanier and M. J. Wagner, *Inorg. Chem.*, 1993, **32**, 833-840.
13. C. P. Love, C. C. Torardi and C. J. Page, *Inorg. Chem.*, 1992, **31**, 1784-1788.
14. M. Hamid, M. Mazhar, Z. Arifin and K. Molloy, *Transition Met. Chem*, 2012, **37**, 241-247.
15. M. Sultan, A. A. Tahir, M. Mazhar, M. Zeller and K. G. U. Wijayantha, *New J. Chem.*, 2012, **36**, 911-917.
16. SAINT, *Area detector integration software*, (1995) Siemens Analytical Instruments Inc., Madison, WI, USA.
17. S. G.M. Sheldrick, *Program for semi-empirical absorption correction*, (1997) University of Göttingen, Göttingen, Germany.
18. G. M. Sheldrick, *Acta Cryst.*, 2008, **A64**, 112-122.
19. A. A. Tahir, K. C. Molloy, M. Mazhar, G. Kociok-Köhn, M. Hamid and S. Dastgir, *Inorg. Chem.*, 2005, **44**, 9207-9212.
20. P. K. Larsen, R. Cuppens and G. A. C. M. Spierings, *Ferroelectrics*, 1992, **128**, 265-292.
21. M. Shahid, M. Hamid, M. Mazhar, J. Akhtar, M. Zeller and A. D. Hunter, *Inorg. Chem. Commun.*, 2011, **14**, 288-291.
22. G. B. Deacon and R. J. Phillips, *Coord. Chem. Rev.*, 1980, **33**, 227-250.
23. B.-H. Ye, X.-Y. Li, I. D. Williams and X.-M. Chen, *Inorg. Chem.*, 2002, **41**, 6426-6431.
24. M. Veith, M. Haas and V. Huch, *Chem. Mater.*, 2004, **17**, 95-101.
25. N. Nawar and N. Hosny, *Transition Met Chem*, 2000, **25**, 1-8.
26. L. Mei, T. Ming, L. Rong, S. Jie, Y. Zhong and L. Liang, *J. Chem. Sci.*, 2009, **121**, 435-440.
27. K. V. Buvaylo EA, Vassilyeva OY, Skelton BW, *Acta Crystallogr. Sect. E Struct. Rep. Online*, 2012, **68**, 2.
28. G. Papadimitropoulos, N. Vourdas, V. E. Vamvakas and D. Davazoglou, *J. Phys.: Conf. Ser.*, 2005, **10**, 182.
29. S. Hong-Tao and S. Yoshio, *Sci. Technol. Adv. Mater.* 2014, **15**, 014205.
30. C. Zhong, H. Ji, R. Li, J. Wang, Z. Li, X. Sun and P. Yang, *RSC Adv.*, 2014, **4**, 6696-6701.
31. S. I. F. YAKUPHANOGLU, M. CAGLAR, Y. CAGLAR, *J. Optoelect. Adv. Mater.*, 2007, **9**, 6.
32. Y. Nakano, S. Saeki and T. Morikawa, *Appl. Phys. Lett.*, 2009, **94**, -.
33. G. H. Li, L. Yang, Y. X. Jin and L. D. Zhang, *Thin Solid Films*, 2000, **368**, 164-167.
34. A. Kudo and Y. Miseki, *Chem. Soc. Rev.*, 2009, **38**, 253-278.
35. R. van de Krol, Y. Liang and J. Schoonman, *J. Mater. Chem.*, 2008, **18**, 2311-2320.